In situ growth of MnO$_2$ nanosheets on honeycomb ceramic via hydrothermal method and its application in catalytic combustion

Fangfang Liu[1], Zehua Xu[1], Yongshen Dou[2], Sanmao Liu[2] and Yongfeng Li*[1,2]

[1] School of Chemical Engineering and Light Industry, Guangdong University of Technology, Guangzhou 510006, PR China

[2] Foshan Shunde Kinglei Environment & Technology Co., LTD, Foshan 528308, PR China

*gdliyf@163.com

Keywords: MnO$_2$ nanosheets, honeycomb ceramic, toluene, monolithic catalyst

Abstract: The manganese oxide (MnO$_2$) nanosheets supported on cordierite honeycomb ceramic (CHC) were synthesized via in-situ growing hydrothermal method. The effects of CH$_3$COOH precursor concentrations on the morphology, crystal structure and toluene purification activity of MnO$_2$/CHC catalyst were mainly investigated. The results revealed that higher CH$_3$COOH concentration of 0.8mol/L will obtain more stable α-MnO$_2$ crystal phase but less exposed MnO$_2$ active surface area in the MnO$_2$/CHC monolithic catalyst. Moreover, the catalyst prepared from 0.8 mol/L CH$_3$COOH concentration exhibits best toluene purification activity, which indicates that the MnO$_2$ crystal structure should play a more important role in catalytic combustion reaction.

Introduction

Volatile organic compounds (VOCs) are the major pollutants in air, which could cause serious harm on human health and environment. There are many kinds of alternative VOC removal technologies and each of them has different limitations. Catalytic combustion is considered as on of the most effective and economical feasible methods to eliminate VOCs emissions[1]. And high-performance catalyst is the key of VOCs catalytic combustion. Nowadays, non-noble metal catalysts have attcacted a lot of attentions due to its low-cost and good thermal priperties[2]. Moreover, the excellent catalytic property of transition metal oxides catalysts, especially MnO$_2$[3, 4], have been proved. However, the MnO$_2$ powder catalyst has come disadvantages, such as being easy to lose and high pressure drop, which limit its industrial application for VOCs purification.

Cordierite honeycomb ceramic (CHC) has been widely used as monolithic supporters or carriers in industry, due to its outsanding thermal and mechanical durability, low pressure drop, and low cost [5]. In this study, the CHC as monolithic substrate was used to support the active component of MnO$_2$ and prepare the high-performance monolithic catalyst by in-situ growing hydrothermal method. And the as-prepared catalysts exhibit good for toluene purification.

Experimental

Preparation of catalyst

Acetic acid (CH$_3$COOH) and potassium permanganate (KMnO$_4$) were used as precursor solution, which could further grow MnO$_2$ nanosheets on the surface of CHC by hydrothermal method. As shown in Fig. 1, the CHC substrate (24 × 5 × 5 mm) was suspended into 25 mL Teflon-lined stainless-steel hydrothermal autoclave with precursor solutions of CH$_3$COOH and KMnO$_4$ under 100°C. After 12h, the catalyst sample was taken out, washed with DI water and dried at 60°C overnight. The obtained monolithic catalyst was denoted as MnO$_2$/CHC.
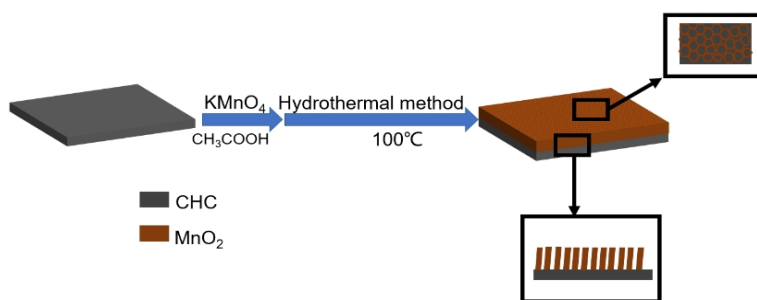
Fig. 1 Schematic diagram of in-situ growth of MnO_2 on CHC substrate via hydrothermal method

Catalytic test

The as-prepared monolithic catalysts were machined to the shape of $5 \times 5 \times 12mm$ and placed in an isothermal fixed-bed continuous-flow reactor with a vertical tubular furnace controlled by a PID controller. The toluene catalytic combustion reactions were performed using toluene/air mixture gas (1.0 g/m^3 toluene in air, 0.1 MPa), at a gas hourly space velocity (GHSV) of 10000 h^{-1}. The inlet feedstocks and outlet products were all analyzed by a gas chromatograph (HP6820, Agilent) with a flame ionization detector (FID). There were no other by-products, except CO_2 and H_2O, being found under our experimental condition.

Characterization

The sample structure was analyzed by scanning electron microscopy (SEM, Hitachi SU8010) with energy dispersive spectrometer (EDS) and power X-ray diffraction (XRD, Rigaku Uitima III Cu Kα).

Results and Discussion

As shown in Fig. 2a, the surface of pure CHC substrate was smooth. In contrast, from the SEM image of as-prepared MnO_2/CHC catalyst (Fig. 2b), it can be observed that the surface of CHC substrate was completely covered by other components. Further from the results of elemental analysis for as-prepared MnO_2/CHC catalyst by EDS in Fig. 3a, there were Mn and O elements being detected, besides the Si, Al ang Mg elements that are attributed to CHC substrate. The EDS result indicates that the MnO_2 active component has been successfully grown on the CHC surface in the MnO_2/CHC catalyst. Moreover, from the high magnification SEM image of the catalyst, in Fig. 2c, it can be found that the MnO_2 component was in the shape of nanosheets on the CHC surface.

The morphology of MnO_2 nanosheets would be affected by the precursor concentrations of CH_3COOH, as shown in Fig. 2(c-e). While using a low CH_3COOH concentration of 0.1mol/L to prepare MnO_2/CHC catalyst, the MnO_2 nanosheets were upright grown and encircled to a porous network structure with the pore size of 30-100 nm on the surface of CHC substrate (in Fig. 2c). When increasing the CH_3COOH concentration to 0.4 mol/L, in the prepared MnO_2/CHC catalyst, some MnO_2 nanosheets were collapsed and began to agglomerate together (in Fig. 2d). Further increasing the CH_3COOH precursor concentration to 0.8 mol/L, all the MnO_2 nanosheets in the prepared MnO_2/CHC catalyst were assembled together to change into irregular ball-like structure on the CHC surface, which results in the decrease of the exposed active surface area of MnO_2 component. Meanwhile, the crystal structure change for the MnO_2/CHC catalysts prepared from different CH_3COOH concentrations was tested by XRD. From Fig. 3b, the sample prepared by low CH_3COOH concentration had diffraction peaks centered at 2θ values of 12.4°, 24.8°, 37.4° and 66.4°, which are in agreement with the standard cards of δ-MnO_2 (JCPDS No. 80-1098)[6]. In contrast, the XRD pattern for the sample prepared from high CH_3COOH concentration of 0.8 mol/L was well correspond to the body-centered tetragonal phase α-MnO_2 (JCPDS No. 44-0141)[7]. The result indicates that increasing CH_3COOH precursor concentration in beneficial to reorganize δ-MnO_2 nanostructure and make the polymorph of MnO_2 transformed to a more stable crystalline phase of α-MnO_2. As a whole, the CH_3COOH precursor concentration could greatly affect the morphology and distribution state of MnO_2 on CHC surface as well as the crystal structure of MnO_2 active component.
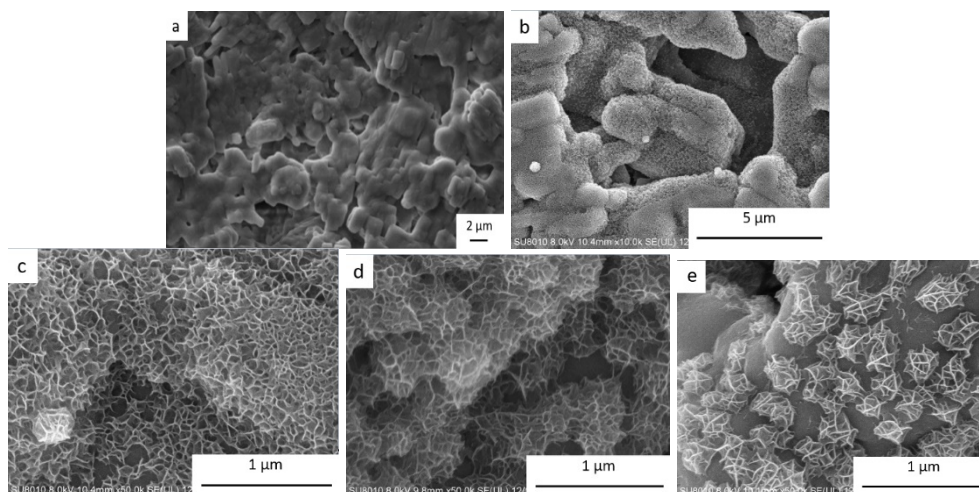
Fig. 2 SEM images of (a) pure CHC substrate and (b-e) MnO$_2$/CHC monolithic catalysts prepared from CH$_3$COOH precursor solution with different concentration of (b, c) 0.1 mol/L, (d) 0.4 mol/L and (e) 0.8 mol/L.
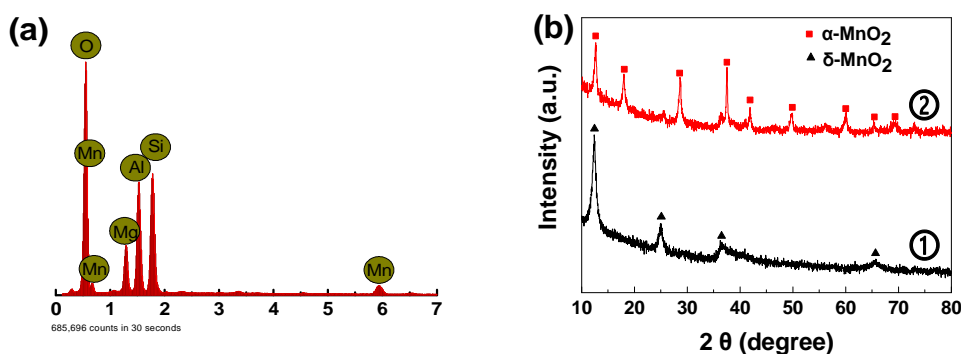

Fig. 3 (a) Element analysis of as-prepared MnO$_2$/CHC catalyst by EDS; (b) XRD spectra of MnO$_2$/CHC monolithic catalysts prepared from CH$_3$COOH precursors with different concentration of ① 0.1 mol/L and ② 0.8 mol/L.

Toluene conversion as a function of reaction temperature on MnO$_2$/CHC monolithic catalysts prepared from different CH$_3$COOH precursor concentrations, are shown in Fig. 4. It can be found that the toluene conversion was 90% at a reaction temperature of 330 °C on the MnO$_2$/CHC catalyst prepared from 0.1 mol/L CH$_3$COOH precursor solution. While increasing the CH$_3$COOH concentration to 0.4 mol/L, on the prepared catalyst, the conversion was only 60% at a reaction temperature of 330 °C. From the SEM results, in Fig. 2c and d, it suggests that the porous network structure with suitable pore size distribution in the MnO$_2$/CHC catalyst prepared from low CH$_3$COOH concentration of 0.1 mol/L could provide more exposed MnO$_2$ active sites to fully contact with reactants, so as to increase the catalytic combustion activity. However, for the MnO$_2$/CHC catalyst prepared from higher CH$_3$COOH precursor concentration of 0.8 mol/L, the toluene conversion reached 90% at a lower temperature of 270 °C. That is to say, although the MnO$_2$/CHC catalyst prepared from 0.8 mol/L CH$_3$COOH concentration has lower expose active surface area than that prepared from 0.1 mol/L CH$_3$COOH concentration (as shown in Fig. 2c and e), it exhibits better catalytic combustion activity. Considering the XRD result in Fig. 3b, it indicates that the α-MnO$_2$ phase is more active than δ-MnO$_2$ phase for MnO$_2$/CHC monolithic catalyst in toluene combustion reaction. Moreover, the results also suggest that the MnO$_2$ crystal structure in MnO$_2$/CHC catalyst might play a more important role on toluene combustion activity, compared to the distribution state of MnO$_2$ on CHC surface.
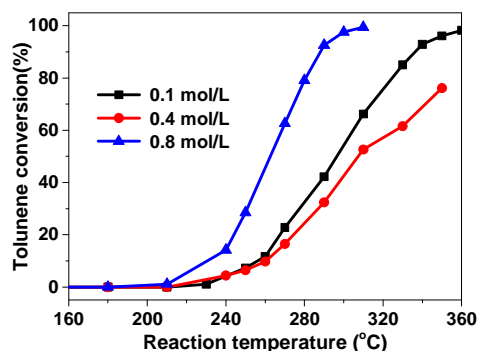
Fig. 4 Toluene conversion as a function of reaction temperature on MnO_2/CHC monolithic catalysts prepared from CH_3COOH precursors with different concentrations.

Conclusions

In this work, in-situ growing MnO_2 nanosheets on CHC were successfully prepared via a facile hydrothermal method. As can be seen from the result of SEM, EDS and XRD, lower precursor concentration of CH_3COOH will obtain the MnO_2/CHC catalyst with more exposed active surface areas. But higher CH_3COOH concentration of 0.8 mol/L will be beneficial to form a α-MnO_2 crystal structure but decrease the exposed active surface area. Because the latter catalyst exhibited greater catalytic property, it indicates that the MnO_2 crystal structure might play a more important role in catalytic combustion reaction, compared to the exposed MnO_2 active surface area.

Acknowledgements

References

[1] W.B. Li, J.X. Wang, H. Gong, Catalysis Today 148 (2009) 81-87.

[2] J.M. Gatica, J. Castiglioni, C. de los Santos, M.P. Yeste, G. Cifredo, M. Torres, H. Vidal, Catalysis Today 296 (2017) 84-94.

[3] J. Hou, Y. Li, M. Mao, L. Ren, X. Zhao, ACS Appl Mater Interfaces 6 (2014) 14981-14987.

[4] J. Jia, W. Yang, P. Zhang, J. Zhang, Applied Catalysis A: General 546 (2017) 79-86.

[5] S.Y. Chen, W. Song, H.J. Lin, S. Wang, S. Biswas, M. Mollahosseini, C.H. Kuo, P.X. Gao, S.L. Suib, ACS Appl Mater Interfaces 8 (2016) 7834-7842.

[6] X. Su, L. Yu, G. Cheng, H. Zhang, M. Sun, L. Zhang, J. Zhang, Applied Energy 134 (2014) 439-445.

[7] J. Jia, P. Zhang, L. Chen, Catalysis Science & Technology 6 (2016) 5841-5847.